

Lagrangian derivation and analysis of a simple equivalent circuit model of wireless power transfer system with dual transmitting resonators

Takahiro Koyama, Toru Honjo, Kazuhiro Umetani, Eiji Hiraki
Okayama University
Tsushima-naka 3-1-1, Kita-ku
Okayama, Japan

Published in: 2016 18th European Conference on Power Electronics and Applications (EPE'16 ECCE Europe)

© 2016 IEEE. Personal use of this material is permitted. Permission from IEEE must be obtained for all other uses, in any current or future media, including reprinting/republishing this material for advertising or promotional purposes, creating new collective works, for resale or redistribution to servers or lists, or reuse of any copyrighted component of this work in other works.

DOI: 10.1109/EPE.2016.7695439

Lagrangian Derivation and Analysis of a Simple Equivalent Circuit Model of Wireless Power Transfer System with Dual Transmitting Resonators

Takahiro Koyama, Toru Honjo, Kazuhiro Umetani, Eiji Hiraki

Okayama University

Tsushima-naka 3-1-1, Kita-ku

Okayama, Japan

Tel.: +81 / (86) – 251.8115.

Fax: +81 / (86) – 251.8258.

E-Mail: pk430kpd@s.okayama-u.ac.jp

URL: <http://www.okayama-u.ac.jp/>

Keywords

«Wireless power transmission», «Efficiency», «Modelling»

Abstract

This paper proposes a novel analysis method for the dual transmitting resonators wireless power transfer (DTR-WPT) system. The DTR-WPT is attractive for its higher efficiency and greater power transfer capability compared with the conventional single transmitting resonator wireless power transfer (STR-WPT) system. However, analytical understanding of the DTR-WPT is difficult due to its complicated operating principle caused by two transmitting resonators and a receiving resonator, which are all magnetically coupled each other. Therefore, practical applications of the DTR-WPT may be hindered by difficulty in establishing a design optimization method and a control scheme.

This difficulty is addressed in this paper by proposing a novel simple equivalent circuit model of the DTR-WPT. Lagrangian dynamics is employed to derive this model. Brief analysis of this model showed improvement in the efficiency and the power transfer capability by the DTR-WPT compared with the conventional STR-WPT. In addition, the power transfer of the DTR-WPT system was found to be expressed by the same equivalent circuit model as the STR-WPT system. Therefore, similar design optimization methods and similar control schemes as for the STR-WPT are applicable to the DTR-WPT. Along with the theory, this paper presents experiments that verified appropriateness of the proposed model as well as the analysis results based on this model.

Introduction

Recently, magnetic-coupling wireless power transfer (WPT) is attracting growing attention as a convenient power supply method to a small medical device inside a human body. For example, capsule endoscopy [1]–[5], or a small capsule containing a small camera inside, is expected to replace gastric camera, which often inflicts great suffering during swallowing the camera. The capsule often contains a battery for power supply. However, the battery can occupy significant volume in the capsule or can limit the operating time. Therefore, power supply to this capsule should be preferably provided from an external power source rather than the battery. For this purpose, WPT is emerging as an attractive and promising field of techniques [1][5].

However, WPT to the capsule may suffer from low efficiency and low power transfer capability because the size of the receiving coil inside the capsule is severely limited. One effective approach to address this issue is to increase magnetic field induction inside the human body.

The dual transmitting resonator wireless power transfer (DTR-WPT) system [6] can be a promising technique for this approach. Figure 1 illustrates the DTR-WPT system in comparison with the conventional single transmitting resonator wireless power transfer (STR-WPT) system[7]–[10]. The DTR-WPT system is composed of two transmitting resonators sandwiching a receiving resonator. One transmitting resonator is supplied with an AC power, whereas the other is an independent resonator without a power supply. The former transmitting resonator excites resonance in the latter

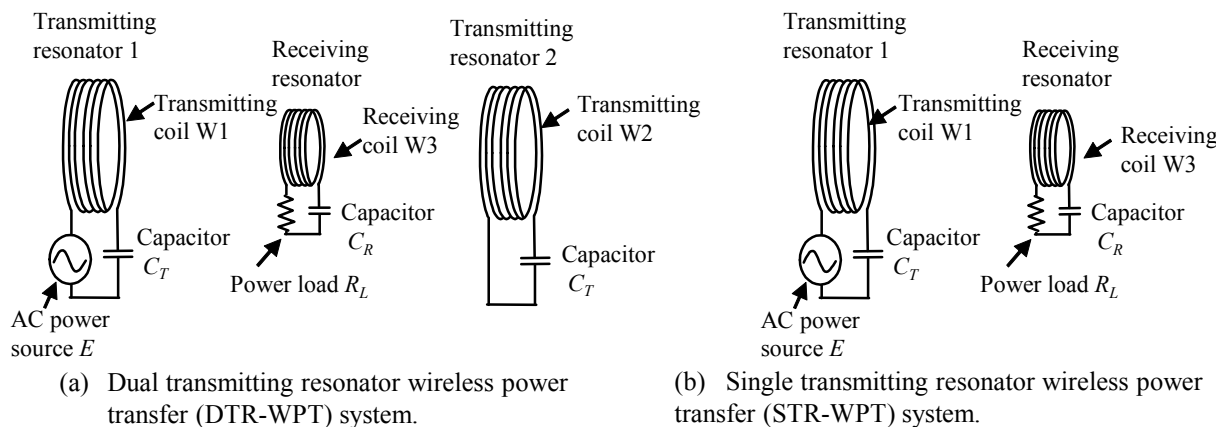


Fig. 1. Physical structures of wireless power transfer systems.

transmitting resonator. As a result, the two transmitting resonators can reinforce the magnetic field at the receiving resonator, if an appropriate resonance mode is excited.

Compared with multi-resonator systems in which all transmitting resonators are connected to the power supply [11][12], the DTR-WPT system is attractive for its convenience, because only one AC power supply suffices to supply the power and the system is free from wire connection between the transmitting resonators. However, operation analysis of the DTR-WPT system tends to be difficult because of complex resonance modes caused by complex magnetic coupling among the three resonators. This difficulty can hinder development of design optimization methods and control schemes for the DTR-WPT system.

In order to address the issue, this paper proposes a novel simple equivalent circuit model of the DTR-WPT system. As a result, this paper elucidates that the power transfer in the DTR-WPT system can be expressed by the same equivalent circuit model as the conventional STR-WPT system. This suggests that similar design optimization methods and similar control schemes as for the STR-WPT system are also applicable to the DTR-WPT system. In addition, brief analysis of the proposed equivalent circuit model shows improvement in the efficiency and the power transfer capability by the DTR-WPT.

The proposed model is derived using Lagrangian model of power electronics [13]–[17]. This derivation method is recently proposed in [15]; and this method was found to derive simple equivalent circuit models [18]–[21] that are often difficult to derive using other methods.

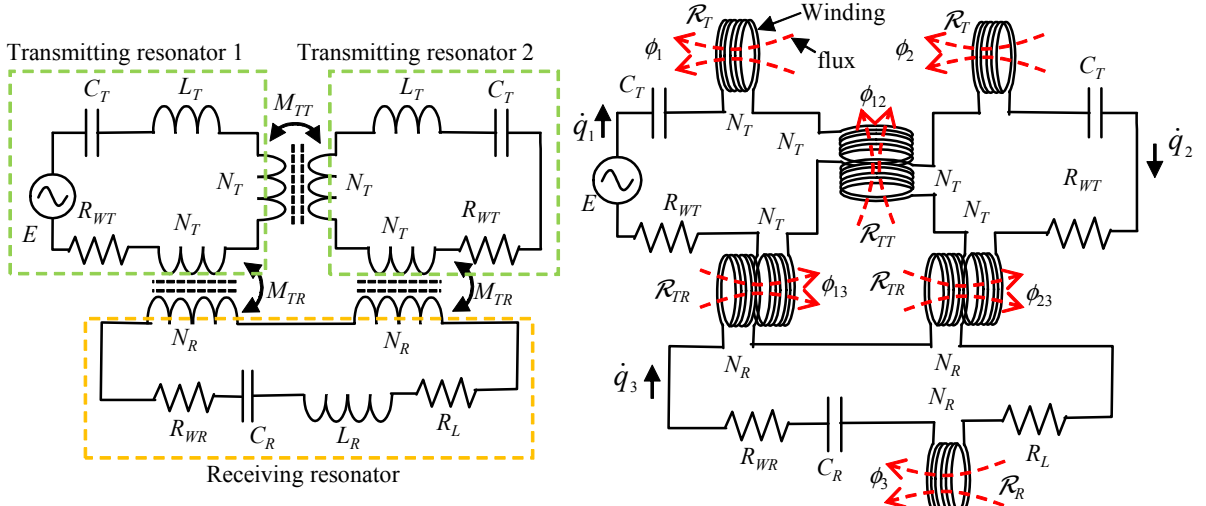
The following discussion is composed of four sections. Section 2 discusses derivation of the proposed equivalent circuit model. Then, section 3 presents brief analysis of the model to show how the DTR-WPT system can improve the efficiency and the power transfer capability. Section 4 presents experiments to verify the proposed model and the analysis results. Finally, section 5 presents the conclusions.

Derivation of Proposed Equivalent Circuit Model

This section derives the proposed equivalent circuit model of the DTR-WPT system using Lagrangian dynamics. The analyzed system is presented in Fig. 1(a). For convenience, the two transmitting resonators are assumed to be symmetric, i.e. transmitting coils W1 and W2 have the same leakage inductance L_T and the parasitic resistance R_{WT} . Furthermore, receiving coil W3 is assumed to be placed at the center between W1 and W2. Hence, the magnetic coupling between W1 and W3 has the same mutual inductance M_{TR} as that between W2 and W3.

The electric behavior of transmitting and receiving coils W1-W3 can be expressed by the circuit model, in which each leakage inductance is represented by an inductor and each mutual inductance is represented by a coupled inductor. Therefore, Fig. 1(a) can be expressed as the circuit model shown in Fig. 2(a), where M_{TT} is the mutual inductance between W1 and W2, L_R and R_{WR} are the leakage inductance and the parasitic resistance of W3, respectively. The number of turns of W1 and W2 is denoted as N_T , whereas that of W3 is denoted as N_R .

Next, Lagrangian model for Fig. 2(a) is constructed. Conventionally, the model is constructed by regarding the energy of inductors as the kinetic energy and the energy of capacitors as the potential



(a) Circuit model with inductors and coupled inductors. (b) Circuit model with magnetic circuits composed of windings, fluxes, and reluctance.

Fig. 2. Circuit models of the dual transmitting resonator wireless power transfer system (DRT-WPT).

energy [13][14]. However, recent studies [15]–[17] have proposed a novel Lagrangian modeling, which improved the conventional modeling to cover the complicated magnetic coupling. Based on this novel Lagrangian modeling, [15] proposed a novel method to derive equivalent circuit models. Recently, [18]–[21] have proven effectiveness of this method because this method was found to derive simple equivalent circuit models that are often difficult to derive using other methods.

This method is applicable to the Lagrangian model constructed from the circuit model, in which all magnetic devices are expressed using magnetic circuits. Therefore, three inductors and three coupled inductors in Fig. 2(a) are expressed as independent magnetic circuits with fluxes $\phi_1, \phi_2, \phi_3, \phi_{12}, \phi_{13}, \phi_{23}$ and reluctance $\mathcal{R}_T, \mathcal{R}_R, \mathcal{R}_{TT}, \mathcal{R}_{TR}$, as shown in Fig. 2(b). Reluctance $\mathcal{R}_T, \mathcal{R}_R, \mathcal{R}_{TT}, \mathcal{R}_{TR}$ are defined as

$$\mathcal{R}_T = N_T^2 / L_T, \quad \mathcal{R}_R = N_R^2 / L_R, \quad \mathcal{R}_{TT} = N_T^2 / M_{TT}, \quad \mathcal{R}_{TR} = N_T N_R / M_{TR}. \quad (1)$$

Derivation of the equivalent circuit model consists of the following three steps. First, the Lagrangian model of Fig. 2(b) is configured. Second, an appropriate co-ordinate transformation is applied to transform the Lagrangian model into another equivalent Lagrangian model belonging to a simpler circuit topology. Third, this equivalent Lagrangian model is translated into a circuit diagram, which is the equivalent circuit model.

Now, we derive the equivalent circuit model of the DTR-WPT system. As reported in literature [15], [17]–[21], the Lagrangian model can be directly configured from the physical circuit structure. Applying the method reported in [15][17], we can obtain the Lagrangian model of Fig. 2(b). Let A and D be the Lagrangian and the dissipation function [22] of the DTR-WPT system. Then, we have

$$\begin{aligned} A = & N_T \dot{q}_1 \phi_1 + N_T \dot{q}_2 \phi_2 + N_R \dot{q}_3 \phi_3 + N_T (\dot{q}_1 + \dot{q}_2) \phi_{12} + (N_T \dot{q}_1 + N_R \dot{q}_3) \phi_{13} \\ & + (N_T \dot{q}_2 + N_R \dot{q}_3) \phi_{23} - \frac{1}{2} \mathcal{R}_T \phi_1^2 - \frac{1}{2} \mathcal{R}_T \phi_2^2 - \frac{1}{2} \mathcal{R}_R \phi_3^2 - \frac{1}{2} \mathcal{R}_{TT} \phi_{12}^2 - \frac{1}{2} \mathcal{R}_{TR} \phi_{13}^2 \\ & - \frac{1}{2} \mathcal{R}_{TR} \phi_{23}^2 - \frac{q_1^2}{2C_T} - \frac{q_2^2}{2C_T} - \frac{q_3^2}{2C_R} + E q_1, \end{aligned} \quad (2)$$

$$D = \frac{1}{2} R_L \dot{q}_3^2 + \frac{1}{2} R_{WT} \dot{q}_1^2 + \frac{1}{2} R_{WT} \dot{q}_2^2 + \frac{1}{2} R_{WR} \dot{q}_3^2, \quad (3)$$

where q_1, q_2 , and q_3 are the time integration of the current flowing through W1–W3, respectively; C_T and C_R are the capacitors in the transmitting and receiving resonators, respectively; E is the voltage of

the AC power supply; and R_L is the load resistance. A dot over a variable indicates its time derivative. Hence, \dot{q}_1 , \dot{q}_2 , and \dot{q}_3 are the current flowing through W1–W3.

Next, a co-ordinate transformation is applied to (2) and (3), as exemplified in [15], [18]–[21]. As a result, another Lagrangian model, which belongs to an equivalent circuit model can be obtained. For this purpose, we introduce imaginary flux ϕ_A , ϕ_B , ϕ_C , and ϕ_D defined as

$$\phi_A = \frac{\phi_1}{\sqrt{2}} + \frac{\phi_2}{\sqrt{2}}, \quad \phi_B = \frac{\phi_1}{\sqrt{2}} - \frac{\phi_2}{\sqrt{2}}, \quad \phi_C = \frac{\phi_{13}}{\sqrt{2}} + \frac{\phi_{23}}{\sqrt{2}}, \quad \phi_D = \frac{\phi_{13}}{\sqrt{2}} - \frac{\phi_{23}}{\sqrt{2}}. \quad (4)$$

Furthermore, we introduce q_A and q_B defined as

$$q_A = \frac{q_1}{\sqrt{2}} + \frac{q_2}{\sqrt{2}}, \quad q_B = \frac{q_1}{\sqrt{2}} - \frac{q_2}{\sqrt{2}}. \quad (5)$$

Eliminating ϕ_1 , ϕ_2 , ϕ_{13} , ϕ_{23} , q_1 , and q_2 , we have

$$\begin{aligned} \mathcal{L} &= \frac{1}{2} N_T (\dot{q}_A + \dot{q}_B) (\phi_A + \phi_B) + \frac{1}{2} N_T (\dot{q}_A - \dot{q}_B) (\phi_A - \phi_B) + N_R \dot{q}_3 \phi_3 + \sqrt{2} N_T \dot{q}_A \phi_{12} \\ &\quad + \frac{1}{2} (N_T \dot{q}_A + N_T \dot{q}_B + \sqrt{2} N_R \dot{q}_3) (\phi_C + \phi_D) + \frac{1}{2} (N_T \dot{q}_A - N_T \dot{q}_B + \sqrt{2} N_R \dot{q}_3) (\phi_C - \phi_D) \\ &\quad - \frac{1}{4} \mathcal{R}_T (\phi_A + \phi_B)^2 - \frac{1}{4} \mathcal{R}_T (\phi_A - \phi_B)^2 - \frac{1}{2} \mathcal{R}_R \phi_3^2 - \frac{1}{2} \mathcal{R}_{TT} \phi_{12}^2 - \frac{1}{4} \mathcal{R}_{TR} (\phi_C + \phi_D)^2 \\ &\quad - \frac{1}{4} \mathcal{R}_{TR} (\phi_C - \phi_D)^2 - \frac{1}{4C_T} (q_A + q_B)^2 - \frac{1}{4C_T} (q_A - q_B)^2 - \frac{q_3^2}{2C_R} + \frac{E}{\sqrt{2}} (q_A + q_B) \\ &= N_T \dot{q}_A \phi_A + N_T \dot{q}_B \phi_B + N_R \dot{q}_3 \phi_3 + \sqrt{2} N_T \dot{q}_A \phi_{12} + (N_T \dot{q}_A + \sqrt{2} N_R \dot{q}_3) \phi_C + N_T \dot{q}_B \phi_D \\ &\quad - \frac{1}{2} \mathcal{R}_T \phi_A^2 - \frac{1}{2} \mathcal{R}_T \phi_B^2 - \frac{1}{2} \mathcal{R}_R \phi_3^2 - \frac{1}{2} \mathcal{R}_{TT} \phi_{12}^2 - \frac{1}{2} \mathcal{R}_{TR} \phi_C^2 - \frac{1}{2} \mathcal{R}_{TR} \phi_D^2 \\ &\quad - \frac{q_A^2}{2C_T} - \frac{q_B^2}{2C_T} - \frac{q_3^2}{2C_R} + \frac{E}{\sqrt{2}} (q_A + q_B), \end{aligned} \quad (6)$$

$$D = \frac{1}{2} R_L \dot{q}_3^2 + \frac{1}{2} R_{wT} \dot{q}_A^2 + \frac{1}{2} R_{wT} \dot{q}_B^2 + \frac{1}{2} R_{wR} \dot{q}_3^2. \quad (7)$$

Translating (6) and (7) into a circuit diagram yields the equivalent circuit model, shown in Fig. 3. Detailed method for translating the Lagrangian model is presented in [15][17].

The equivalent circuit model consists of two independent circuits, i.e. circuits A and B. Compared with the original circuit model, i.e. Fig. 2(a), the equivalent circuit model is simple because there is only one single transformer and three inductors without complicated magnetic coupling. Note that the transformer in the equivalent circuit model does not directly correspond to the transmitting and receiving coils, i.e. W1 and W3. Actually, the turn ratio of the transformer is different from that between W1 and W3.

Circuit A contains the current \dot{q}_A , which is proportional to the average current of W1 and W2; and circuit B contains the current \dot{q}_B , which is proportional to the difference current between W1 and W2. Circuit B does not contribute to the power transfer. It should be noted that the co-ordinate transformation in the Lagrangian model conserves the energy. Therefore, the total power supplied from the AC power supply, as well as the power output to the load, is the same between the equivalent circuit model and the original DTR-WPT system.

On the other hand, the conventional STR-WPT system is expressed by the circuit model shown in Fig. 4 by representing each leakage inductance by an inductor and each mutual inductance by a

coupled inductor. Therefore, circuit A in Fig. 3 has the same circuit topology as the conventional STR-WPT system. The only difference between circuit A and Fig. 4 is the following circuit parameters:

1. Equivalent leakage inductance of the primary side,
2. Equivalent mutual inductance between the primary and secondary sides,
3. Equivalent number of turns in the secondary side.

Note that Fig. 3 is obtained under assumption that W3 is placed at the center between W1 and W2. Therefore, this equivalency of the circuit topology between circuit A and Fig. 4 indicates that the power transfer in the DTR-WPT system can be discussed similarly as in the STR-WPT system in which the abovementioned three circuit parameters are changed appropriately, as far as the receiving coil is placed at the center between the two transmitting coils. Therefore, the DTR-WPT can be optimized by applying the design optimization methods and the control schemes for the STR-WPT system to circuit A.

Analysis of Proposed Equivalent Circuit Model

The proposed equivalent circuit model can be analyzed comparatively easily to show how the DTR-WPT is beneficial compared with the conventional STR-WPT. This section presents brief analysis to elucidate that the DTR-WPT can improve the efficiency and the power transfer capability in power supply to small medical devices inside the human body.

In this analysis, we introduce the following three assumptions:

1. M_{TT} and M_{TR} are far smaller than L_T and L_R . Specifically, $2M_{TT} \ll L_T$, $N_T M_{TR} / N_R \ll L_T$, and $N_R M_{TR} / N_T \ll L_R$.
2. M_{TT} is designed large enough to separate the resonance frequency of circuit A from that of circuit B. Therefore, the current in circuit B is far smaller than the primary current in circuit A, when circuit A is in the resonance.
3. ωM_{TR} is far smaller than $N_R R_{WT} / N_T$, where ω is the angular frequency of the AC power supply.

Generally, the mutual inductance is far smaller than leakage inductance in practical wireless power transfer systems. Therefore, assumption 1 can be expected to be satisfied in many practical designs. In the applications of power supply to medical devices inside the human body, the transmitting coils are often designed to cover the width of the human body; and these coils are placed closely to sandwich

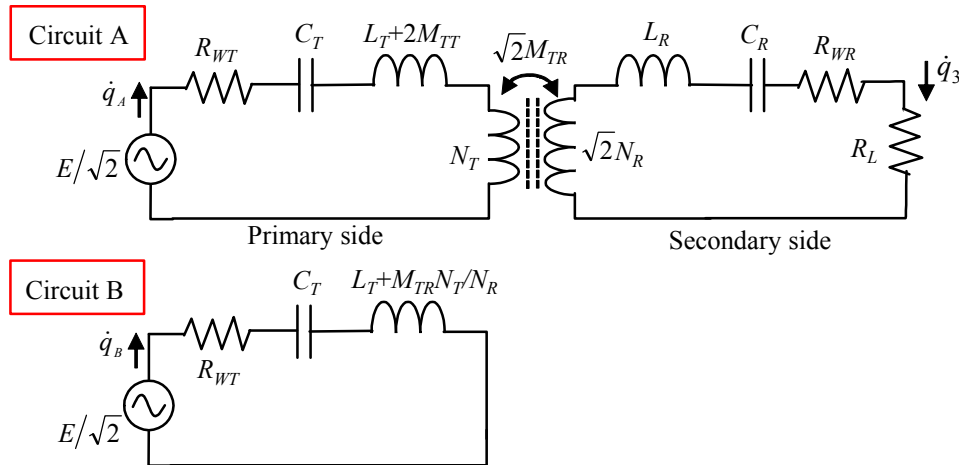


Fig. 3. Equivalent circuit model of the dual transmitting resonator wireless power transfer (DTR-WPT) system.

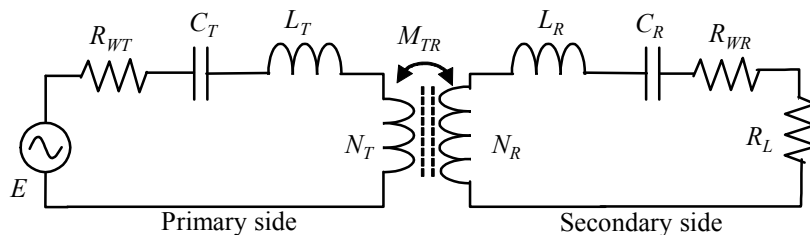


Fig. 4. Equivalent circuit model of the single transmitting resonator wireless power transfer (STR-WPT) system.

the body. Therefore, assumption 2 can be expected to be satisfied in many practical designs. In addition, because of the limited size of the receiving coil, ωM_{TR} tends to be far smaller than the impedance of the transmitting resonators. Hence, assumption 3 can also be expected to be satisfied in many practical designs.

First, we compare the efficiency between the DTR-WPT and STR-WPT systems. As can be seen in Fig. 3, the power can be effectively transferred to the load when circuit A is in the resonance. Therefore, the AC power supply is assumed to operate at such a frequency that excites resonance in circuit A. Then, according to assumption 2, the power loss in circuit B can be neglected compared with that in circuit A because the current flowing in circuit B is assumed to be far smaller than the primary current in circuit A. As a result, the efficiency of the DTR-WPT system can be approximated as the efficiency of circuit A in Fig. 3.

As widely known, the maximum efficiency of the STR-WPT system can be determined by the figure-of-merit [23], defined as $k^2 Q_1 Q_2$, where k is the magnetic coupling coefficient, and Q_1 and Q_2 are the Q values of the transmitting and receiving resonators, respectively. According to assumption 1, the self-inductance of the primary side of circuit A, i.e. $L_T + 2M_{TT} + N_T M_{TR} / N_R$ is almost the same as that in Fig. 4, i.e. $L_T + N_T M_{TR} / N_R$. In addition, the self-inductance of the secondary side of circuit A, i.e. $L_R + 2N_R M_{TR} / N_T$ is almost the same as that in Fig. 4, i.e. $L_R + N_R M_{TR} / N_T$. Therefore, Q_1 and Q_2 are almost the same between circuit A and Fig. 4. On the other hand, k in circuit A is $\sqrt{2}$ times as large as that in Fig. 4, because k is approximated as $\sqrt{2} M_{TR} / \sqrt{L_T L_R}$ in circuit A and $M_{TR} / \sqrt{L_T L_R}$ in Fig. 4. As a result, circuit A can approximately double the figure-of-merit. Consequently, the DTR-WPT system can improve the efficiency compared with the STR-WPT system.

Next, we compare the power transfer capability between the DTR-WPT and STR-WPT systems. Certainly, the DTR-WPT system may require an AC power supply with larger voltage amplitude than the STR-WPT system in order to achieve the same primary current in circuit A as in Fig. 4, because the voltage of the equivalent power supply in circuit A is $1/\sqrt{2}$ of the voltage of the actual AC power supply in the DTR-WPT system. However, this does not limit the maximum output power, if the voltage of the AC power supply can be designed freely. In this case, the maximum output power is generally limited by the maximum voltage stress in the capacitor. In other words, the maximum output power is limited by the maximum allowable current in the transmitting coil, which determines the required voltage stress of the capacitor. Therefore, in this paper, the power transfer capability is defined as the maximum output power under given maximum transmitting coil current.

The transmitting coil current of the DTR-WPT system is $1/\sqrt{2}$ of the primary current in circuit A of Fig. 3, because transmitting coil current \dot{q}_1 and \dot{q}_2 are defined as $\dot{q}_1 = \dot{q}_A / \sqrt{2} + \dot{q}_B / \sqrt{2}$ and $\dot{q}_2 = \dot{q}_A / \sqrt{2} - \dot{q}_B / \sqrt{2}$, respectively. (Note that \dot{q}_B is assumed to be ignorable compared with \dot{q}_A according to assumption 2.) Therefore, the transmitting coil current in the DTR-WPT system is approximately $1/\sqrt{2}$ of that in the STR-WPT system under the condition of the same primary current in circuit A and Fig. 4. In other words, the primary current of circuit A is $\sqrt{2}$ times as large as that of Fig. 4, if the same transmitting coil current is applied to the DTR-WPT and STR-WPT systems.

Furthermore, circuit A in Fig. 3 can transfer larger power than Fig. 4, even if compared under the condition of the same primary current. The reason is discussed below. As discussed above, the efficiency of circuit A is higher than Fig. 4. Therefore, the power loss of circuit A is smaller than that of Fig. 4, if compared under the same output energy. This indicates that the power loss of circuit A is smaller under the condition of the same secondary current, because the resistance of the output load is the same between circuit A and Fig. 4. Note that the parasitic resistance of the primary and secondary sides are also the same between circuit A and Fig. 4. Hence, the primary current in circuit A must be smaller than Fig. 4 under the condition of the same secondary current. In other words, circuit A can transfer larger output power under the condition of the same primary current.

Consequently, the DTR-WPT system can improve the power transfer capability compared with the STR-WPT system.

This improvement in the power transfer capability can be quantitatively estimated, if we consider assumption 3. For this purpose, circuit A and Fig. 4 are further simplified by expressing the transformers using ideal transformers and inductors. Figure 5 presents the result. Now, we assume that

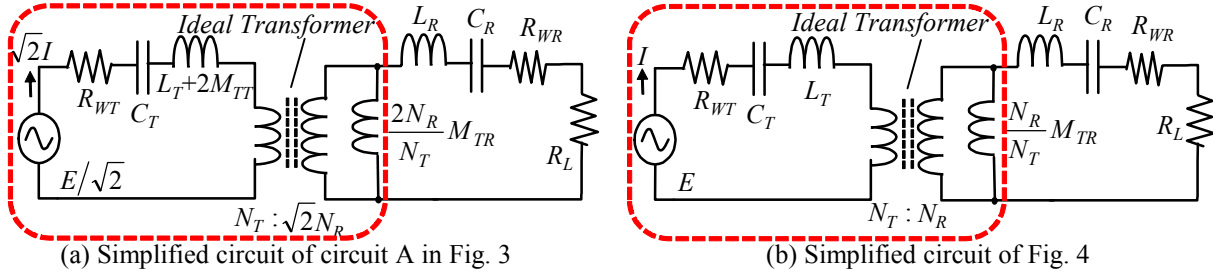


Fig. 5. Simplified circuits of circuit A and Fig. 4 obtained by expressing a transformer using an ideal transformer and an inductor.

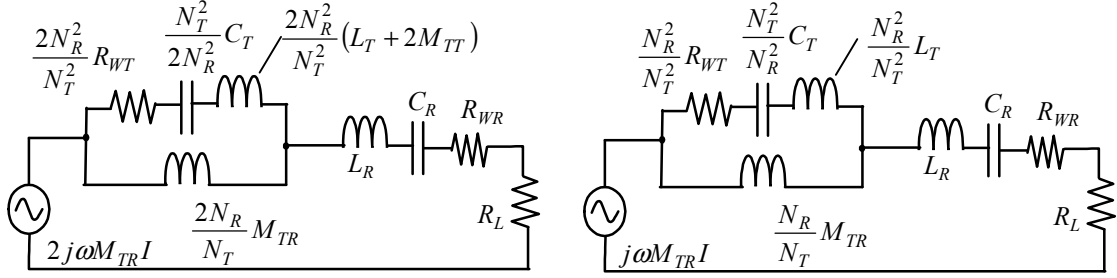


Fig. 6. Further simplified circuits of Fig. 5.

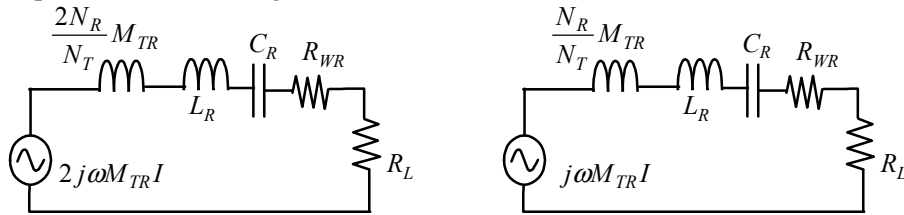


Fig. 7. Approximated circuits of Fig. 6.

the same transmitting coil current flows in the DTR-WPT and STR-WPT systems; and therefore, the primary current of Fig. 5(a) is $\sqrt{2}$ times as large as that of Fig. 5(b) according to the above discussion. (In Fig. 5, the transmitting coil current is denoted as I .) Applying Thevenin's theorem to the subcircuits marked by the dashed boxes in Fig. 5, we can express Fig. 5 as the simplified circuit models shown in Fig. 6. Because of assumptions 3, we can ignore the parallel connection of the impedance of the primary side. Hence, Fig. 6 can be further approximated as Fig. 7.

Fig. 7(a) and Fig. 7(b) has the same topology with the same circuit parameters except for the inductance and the voltage of the AC power supply. Because difference in the inductance does not affect the amplitude of the current at the resonance frequency of these equivalent circuit models, the current is doubled in Fig. 7(a) compared with Fig. 7(b). Therefore, the output power to the load in Fig. 7(a) is 4 times as large as that in Fig. 7(b). Note that the output power to the load in Fig. 7(a) and Fig. 7(b) are approximations of that in the DTR-WPT and STR-WPT systems, respectively. Consequently, the maximum output power of the DTR-WPT system is approximately 4 times as large as that of the STR-WPT system, if compared under the condition of the same transmitting coil current, or the condition of the same voltage stress of the capacitors.

Experiment

Experiment was carried out to verify the proposed equivalent circuit model and the analysis results. For this purpose, we evaluated the efficiency and the power transfer capability of the DTR-WPT and STR-WPT systems. The measurement results for the DTR-WPT system was compared with the theoretical estimation based on Fig. 3 to confirm appropriateness of the proposed model. In addition, consistency between the experimental results and the analysis results was investigated to confirm the appropriateness of the analysis results.

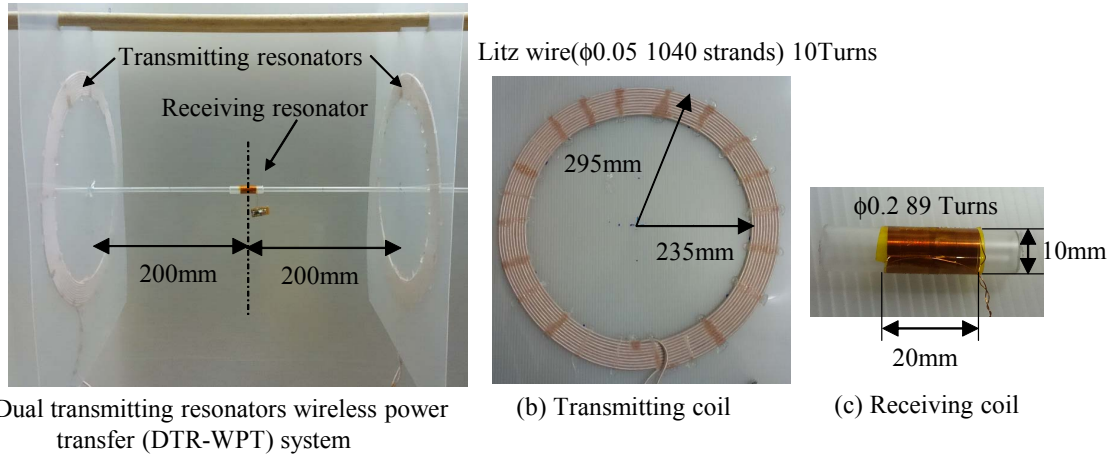


Fig. 8. Photographs of the experimental DTR-WPT system.

Table I: Specifications of the experimental DTR-WPT system

	Transmitting resonators	Receiving resonators
Coil diameter	Inner: 470mm, Outer: 590mm	10mm
Number of turns	10 Turns	89 Turns
Parasitic Resistance	0.576Ω	3.09Ω
Self-inductance	51.7μH	34.5μH
Capacitance	678pF	1.03nF

Mutual inductance between transmitting resonators: 0.701μH
 Mutual inductance between transmitting and receiving resonators: 56.9nH

Figure 8 shows the experimental DTR-WPT system employed for the experiment. The experimental system is composed of two large transmitting coils and a small receiving coil. Capacitors of the transmitting and receiving resonators are designed to have the same resonance frequency of 850kHz. The two transmitting coils are designed the same. One transmitting resonator is connected to the AC power amplifier to supply sinusoidal voltage, whereas the other transmitting resonator is short-circuited. In addition, the receiving resonator is connected to a load resistor. As for the experiment of STR-WPT, we removed the short-circuited transmitting resonator.

Specifications of the experimental DTR-WPT system is presented in Table I. Table I indicates that assumptions 1 and 3 employed in the analysis are satisfied in the experiment. In addition, assumption 2 is also satisfied according to the following reason. The total impedance of the resonator of circuit B in Fig. 3 is estimated as 8Ω approximately at the resonance frequency of circuit A, i.e. 845kHz. On the other hand, the total impedance of circuit A is estimated to be smaller than 0.6Ω at this resonance frequency, regardless to the load resistance. Therefore, the current in circuit B is expected to be far smaller than the primary current in circuit A. Consequently, this experiment can test the analysis results of the previous section because all the three assumptions are satisfied.

Efficiency

First, we evaluated the efficiency of the DTR-WPT and STR-WPT systems. In this experiment, the load resistance R_L was designed so that the experimental systems can achieve the maximum efficiency. The load resistance for the maximum efficiency in the experimental DTR-WPT and STR-WPT systems was determined by numerical calculation based on the theoretical formula [24], which predicts the efficiency of the STR-WPT system, applied to circuit A and Fig. 4, respectively. As a result, R_L was set at 3.2Ω in both the DTR-WPT and STR-WPT systems. Because the experimental systems are composed as linear circuits, the efficiency does not depend on the amplitude of the current from the power supply. However, we set the voltage amplitude of the AC power supply so that the transmitting coil current is kept at 1Arms. (In the DTR-WPT system, we kept the current at 1Arm in the transmitting coil with larger current.)

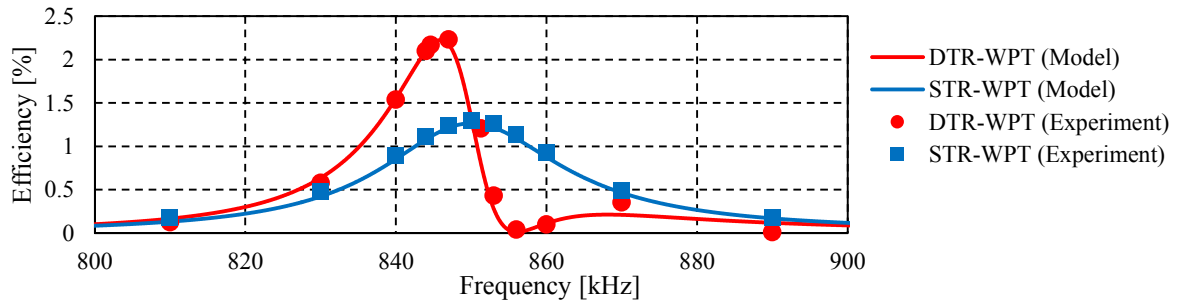


Fig. 9. Experimental results of the efficiency of the DTR-WPT and STR-WPT systems.

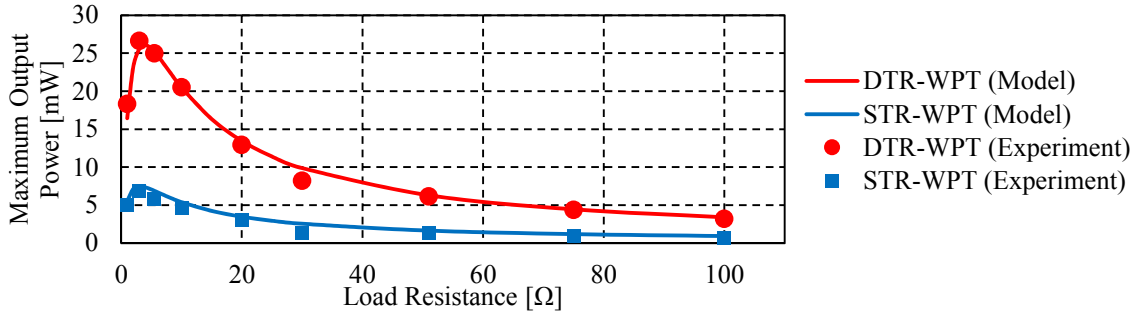


Fig. 10. Experimental results of the maximum output power of the DTR-WPT and STR-WPT systems.

The result is presented in Fig. 9. The result shows that the proposed equivalent circuit model well predicted the efficiency. Furthermore, the DTR-WPT system is found to show higher efficiency than the STR-WPT system, which is consistent with the analysis result.

Power Transfer Capability

Second, we evaluated the maximum output power of the DTR-WPT and STR-WPT systems under the maximum transmitting coil current of 1Arms. In this experiment, we measured the dependency of the output power on the load resistance. For each value of the load resistance, the frequency of the AC power supply was arranged so that the output power can be maximized under the maximum transmitting coil current of 1Arms. As a result, the frequency of the DTR-WPT system was set at 845.2kHz–845.9kHz, whereas that of the STR-WPT was set at 849.0kHz–849.5kHz.

The result is presented in Fig. 10. The result shows that the proposed model also successfully predicted the maximum output power. Furthermore, the DTR-WPT system showed greater maximum output power than the STR-WPT system, regardless to the load resistance. The maximum output power of the DTR-WPT system was approximately 4 times as large as that of the STR-WPT system, which is also consistent with the analysis result.

Consequently, this experiment supported appropriateness of the proposed equivalent circuit model as well as the analysis results.

Conclusion

The DTR-WPT system is expected to improve the efficiency and the power transfer capability in wireless power transfer to small medical devices inside the human body. However, the complex operating principle with multiple resonance modes can hinder analytical understanding of the operation of the system. In order to promote development of design optimization methods and control schemes of the DTR-WPT system, this paper proposed a novel simple equivalent circuit model of the system. As a result, power transfer in the DTR-WPT system is found to be expressed by the same equivalent circuit model as the conventional STR-WPT system. Therefore, similar design optimization methods and similar control schemes as for the STR-WPT system is also applicable to the DTR-WPT system. The proposed equivalent circuit model also revealed merits of the DTR-WPT system in improving the efficiency and the power transfer capability, supporting the usefulness of the DTR-WPT system in applications of small medical devices.

References

- [1] Mackiewicz M., Berens J., Fisher M.: Wireless capsule endoscopy color video segmentation, *IEEE Trans. Med. Imag.*, vol. 27, no. 12, pp. 1769–1781.
- [2] Ciuti G., Menciassi A., Dario P.: Capsule endoscopy: from current achievements to open challenges, *IEEE Rev. Biomed. Eng.*, vol. 4, pp. 59–72.
- [3] Demosthenou P., Constantinou P., Georgiou J.: Infrared fluorescence-based cancer screening capsule for the small intestine, *IEEE Trans. Biomed. Circuit Syst.*, vol. 10, no. 2, pp. 467–476.
- [4] Liu L., Towfighian S., Hila A.: A review of locomotion systems for capsule endoscopy, *IEEE Rev. Biomed. Eng.*, vol. 5, pp. 138–151.
- [5] Woods S. P., Constandinou, T. G.: Wireless capsule endoscopy for targeted drug delivery: mechanics and design considerations, *IEEE Trans. Biomed. Eng.*, vol. 60, no. 4, pp. 945–953.
- [6] Itoh R., Sawahara Y., Ishizaki T., Awai I.: Construction of a secure wireless power transfer system for robot fish, *Proc. IEEE Wireless Power Transfer Conf. 2015*, F3.6, pp. 1–4.
- [7] Jang Y., Jonvanovic M. M.: A contactless electrical energy transmission system for portable-telephone battery chargers, *IEEE Trans. Ind. Electron.*, vol. 50, no. 3, pp. 520–527.
- [8] Cheon S., Kim Y.-H., Kang S.-Y., Lee M. L., Lee J.-M., Zyung T.: Circuit-model-based analysis of a wireless energy-transfer system via coupled magnetic resonances, *IEEE Trans. Ind. Electron.*, vol. 58, no. 7, pp. 2906–2914.
- [9] Li S., Mi C. C.: Wireless power transfer for electric vehicle applications, *IEEE J. Emerg. Sel. Topics Power Electron.*, vol. 3, no. 1, pp. 4–16.
- [10] Zuo W., Wang S., Liao Y., Xu Y.: Investigation of efficiency and load characteristics of superconducting wireless power transfer systems, *IEEE Trans. Appl. Superconductivity*, vol. 25, no. 3, 5000106.
- [11] Nguyen M. Q., Chou Y., Plesa D., Rao S., Chiao J. C.: Multiple-inputs and multiple-outputs wireless power combining and delivering systems, *IEEE Trans. Power Electron.*, vol. 30, no. 11, pp. 6254–6263.
- [12] Koh K. E., Song K., Sukprasert P., Imura T., Hori Y.: Two-transmitter wireless power transfer with LCL circuit for continuous power in dynamic charging, *Proc. 2015 IEEE PELS Workshop on Emerging Technologies: Wireless Power (WoW)*, pp. 1–6.
- [13] Wells D. A.: *Shaum's outline of theory and problems of Lagrangian dynamics*, McGraw-Hill, New York, USA, 1976, pp. 303.
- [14] Sherpen J. M. A., Jeltsema D., Klaasens J. B.: Lagrangian modeling of switched electrical networks, *Syst. Ctrl. Lett.*, vol. 48, pp. 365–374.
- [15] Umetani K.: A generalized method of Lagrangian modeling of power conversion circuit with integrated magnetic components, *IEEJ Trans. Elect. Electron. Eng.*, vol. 7, issue S1, pp. S146–S152.
- [16] Umetani K., Yamamoto M., Hiraki E.: Simple flux-based Lagrangian formulation to model the non-linearity of concentrated-winding switched reluctance motors, vol. 51, no. 24, pp. 1984-1986.
- [17] Umetani K.: Lagrangian-method for deriving electrically dual power converters applicable to non-planar circuit topologies, *IEEJ Trans. Elect. Electron. Eng.*, vol. 11, no. 4. (in press)
- [18] Umetani K., Imaoka J., Yamamoto M., Arimura S., Hirano T.: Evaluation of the Lagrangian method for deriving equivalent circuits of integrated magnetic components: a case study using the integrated winding coupled inductor, *IEEE Trans. Ind. Appl.*, vol. 51, no. 1, pp. 547–555.
- [19] Umetani K., Tera T., Shirakawa K.: A magnetic structure integrating differential-mode and common-mode inductors with improved tolerance to DC saturation, *IEEJ J. Ind. Appl.*, vol. 4, no. 3, pp. 166–173.
- [20] Umegami H., Umetani K., Yamamoto M., Hiraki E.: Lagrangian-based equivalent circuit of basic electric-field coupling wireless power transfer systems, *IEEJ Trans. Elect. Electron. Eng.*, vol. 10, no. S1, pp. S168–S170.
- [21] Umetani K., Hiraki E., Yamamoto M.: Lagrangian-based derivation of a novel sliding mode control for synchronous buck converters, *IEEJ J. Ind. Appl.*, vol. 4, no. 6, pp. 728–729.
- [22] Landau L. D., Lifshitz E. M.: *Mechanics*, Butterworth-Heinemann, 1976, pp.74–77.
- [23] Pinuela M., Yates D. C., Lucyszyn S., Mitcheson P. D.: Maximising DC to load efficiency for inductive power transfer, *IEEE Trans. Power Electron.*, vol. 28, no. 5, pp. 2437–2447.
- [24] Awai I.: Basic characteristic of “Magnetic resonance” wireless power transfer system excited by a 0 ohm power source, *IEICE Electron. Express*, vol. 10, no. 21, pp. 1–13.